Project no. GOCE-CT-2003-505539

Project acronym: ENSEMBLES

Project title: ENSEMBLE-based Predictions of Climate Changes and their Impacts

Instrument: Integrated Project

Thematic Priority: Global Change and Ecosystems

D5.21
Preliminary evaluation of precipitation extremes in RCM data for the Rhine basin

Due date of deliverable: May 2008 (month 45)
Actual submission date: July 2008

Start date of project: 1 September 2004 Duration: 60 Months

Organisation name of lead contractor for this deliverable: KNMI

Project co-funded by the European Commission within the Sixth Framework Programme (2002-2006)		
Dissemination Level		
PU	Public	X
PP	Restricted to other programme participants (including the Commission Services)	
RE	Restricted to a group specified by the consortium (including the Commission Services)	
CO	Confidential, only for members of the Consortium (including the Commission Services)	

ENSEMBLES WP5.4

D5.21

Preliminary evaluation of precipitation extremes in RCM data for the Rhine basin

Martin Hanel and Adri Buishand

Royal Netherlands Meteorological Institute (KNMI)

1. Introduction

A large number of RCM simulations have been performed in the ENSEMBLES project. The assessment of the extremes in these simulations is the objective of work package WP5.4. This report presents an extreme-value model for the evaluation of precipitation extremes in transient RCM simulations. The model is applied to daily precipitation for the river Rhine basin in the RACMO-ECHAM5 simulation.

Precipitation extremes in RCM simulations have been analysed in different ways. One method is to consider the change in a large empirical quantile of the daily precipitation amounts (e.g., the 99th) or the properties of the exceedances of such a quantile (e.g., *Durman et al., 2001*; *Christensen and Christensen, 2004*). An alternative is to fit an extreme-value distribution to the largest daily precipitation amount in a season (e.g., *Frei et al., 2006*; *Goubanova and Li, 2007*) or year (e.g., *Huntingford et al., 2003; Fowler et al., 2005*; *Ekström et al., 2005*). A number of these studies also deal with the maxima of multi-day precipitation amounts.

A problem with extreme precipitation is that the likelihood of detecting a systematic change at a grid box is generally small due to the large year-to-year variability. *Frei and Schär (2001)* mention, for instance, that a frequency change by a factor of 1.5 in events with an average return period of 100 days can be detected with a probability of only 0.2 in a 100-year record. The decrease of this probability with increasing event magnitude limits the detection of systematic changes in extreme events at a single grid box.

Spatial pooling has been considered to obtain meaningful changes in extremes. *Frei et al. (2006)* and *Goubanova and Li (2007)* averaged an estimated quantile of the extreme-value distribution over large regions. An alternative is to assume that the most uncertain parameters of the extreme-value distribution are constant over some region. The estimates of these parameters based on the pooled data across the region are then generally more accurate than those from the data of an individual grid box leading to a reduction of the standard errors of the estimated quantiles of the distribution. This approach has its origin in hydrology where it is known as regional frequency analysis. The most popular method is the index-flood method. *Fowler et al. (2005)* and *Ekström et al. (2005)* applied this method to the 1-, 2-, 5- and 10-day annual maximum precipitation amounts across the UK in two RCM simulations. Apart from a change in the distribution parameters between the control and future climate, these parameters do not vary over time in their application.

In this report an index-flood model with time-varying parameters is presented. The application to the maxima of the simulated daily summer (JJA) precipitation amounts for the Rhine basin is discussed in some detail. The main results for the 5-day winter (DJF) maxima are also briefly mentioned.

The index-flood model is described in Section 2. Section 3 provides some information about the river Rhine basin and the RACMO-ECHAM5 simulation. The results for the summer maxima are presented in Section 4 and those for the winter maxima in Section 5.

2.1 Index-flood model

The idea behind the index-flood method is that the variables within a homogeneous region are identically distributed after scaling with a site-specific factor – the index flood. Then the *T*-year quantile $Q_T(s)$ at any given location *s*, i.e., the value that is exceeded with probability $1/T$, can be written as

$$Q_T(s) = \mu(s) \cdot q_T , \tag{1}$$

where $\mu(s)$ is the index flood and q_T a regional dimensionless quantile function, in this context often called the growth curve. The mean or median of the distribution is usually chosen as the index flood.

The index-flood method has been used with different probability distributions. For seasonal and annual precipitation maxima the generalized extreme value (GEV) distribution is quite popular. This distribution is a three-parameter distribution that combines the three possible types of extreme value distributions (i.e., Gumbel, Fréchet and reverse Weibull distributions). Its distribution function is given by

$$\begin{aligned} F(x) &= \exp\left\{ -\left[1 + \kappa \cdot \left(\frac{x-\xi}{\alpha} \right) \right]^{-\frac{1}{\kappa}} \right\}, && \kappa \neq 0 , \\ F(x) &= \exp\left\{ -\exp\left[-\left(\frac{x-\xi}{\alpha} \right) \right] \right\}, && \kappa = 0 , \end{aligned} \tag{2}$$

with ξ, α and κ the location, the scale and the shape parameter, respectively. The shape parameter controls the behaviour of the tails of the distribution – positive values imply a heavy upper tail (Fréchet distribution).

Apart from support from extreme value theory to select the GEV distribution, it has often been found that this distribution describes the distribution of observed or simulated precipitation maxima well. For annual precipitation maxima of various durations *Schaefer (1990)*, *Alia (1999)* and *Kyselý and Picek (2007),* using L-moment ratio diagrams, observed that the GEV distribution is generally superior to other candidate distributions. In addition, *Alia (1999)* and *Kyselý and Picek (2007)* found that a goodness-of-fit test based on the L-kurtosis did not reject the GEV distribution. *Buonomo et al. (2007)* and *Goubanova and Li (2007)* used the Kolmogorov-Smirnov goodness-of-fit test and concluded that the GEV distribution is appropriate for modelling precipitation extremes in RCM projections for most parts of Europe as well. However, problems were met in dry areas where most of the seasonal maxima were zero.

Scaling a $\mathrm{GEV}(\xi, \alpha, \kappa)$ variable by the mean or median μ results in a $\mathrm{GEV}(\xi/\mu, \alpha/\mu, \kappa)$ variable. The ratios ξ/μ and α/μ are entirely specified by the dispersion coefficient $\gamma = \alpha/\xi$ and κ. Therefore, the parameters γ and κ determine the GEV distribution of the scaled maxima and the growth curve. These parameters are constant over the region in the index-flood method. The dispersion coefficient γ is comparable to the coefficient of variation.

For the development of our non-stationary model it is convenient to use the location parameter as the index flood, i.e., $\mu(s) = \xi(s)$. The growth curve q_T in Eq.(1) then becomes

$$q_T = 1 - \frac{\gamma}{\kappa} \cdot \left\{ 1 - \left[-\log\left(1 - \frac{1}{T}\right) \right]^{-\kappa} \right\}, \qquad \kappa \neq 0,$$
$$q_T = 1 - \gamma \cdot \log\left[-\log\left(1 - \frac{1}{T}\right) \right], \qquad \kappa = 0. \tag{3}$$

Note that $q_T = 1$ for $T = 1/(1-1/e) = 1.58$ years being the return period corresponding to the location parameter.

2.2 Non-stationary index-flood model

A few studies in the hydrological literature deal with non-stationarity in regional frequency analysis. *Cunderlik and Burn (2003)* assume temporal and spatial variation in both the location and scale parameter of the distribution. Linear trends in these parameters were estimated with a distribution-free method due to *Sen (1968)*. In a subsequent paper (*Cunderlik and Ouarda, 2006*) the scale parameter was assumed to be constant over the region of interest but still time-varying. The regional scale parameter was estimated as a weighted average of the at-site scale parameters. *Renard et al. (2006)* used a regional non-stationary GEV model to describe trends in annual maximum discharges. In that model the shape parameter was constant but the scale and location parameters varied over the region and there was a common linear trend in the location parameter. Statistical inference was based on a Bayesian analysis using Markov chain Monte Carlo methods. Other authors have successfully used a GEV distribution with time-varying parameters, e.g., *Kharin and Zwiers (2005)*, *Adlouni et al. (2007)* and *García et al. (2007)*, although not in the framework of regional frequency analysis.

Using the location parameter of the GEV distribution as the index flood, the *T*-year quantile at location *s* in year *t* can be represented as

$$Q_T(s,t) = \xi(s,t) \cdot q_T(t), \tag{4}$$

where $q_T(t)$ is given by Eq.(3) but with time-dependent dispersion coefficient $\gamma(t)$ and shape parameter $\kappa(t)$. The location parameter $\xi(s,t)$ varies both in time and space.

We propose the following model for the parameters:

$$\xi(s,t) = \xi_0(s) \cdot \exp\left[\xi_1 \cdot (t - t_0)_+ \right] \tag{5}$$

$$\gamma(t) = \gamma_0 \cdot \exp\left[\gamma_1 \cdot (t - t_0)_+ \right] \tag{6}$$

$$\kappa(t) = \kappa_0 + \kappa_1 \cdot (t - t_0)_+ \tag{7}$$

where t_0 is the start of the trend and $(\cdot)_+ = \max(\cdot, 0)$.

In line with GEV models with a time-dependent scale parameter, the exponential function is used in Eq.(6) to avoid negative values of the dispersion coefficient. An exponential function is also used in Eq.(5) for the location parameter to achieve that the

relative changes of the quantiles are constant over the region of interest. From Eq.(4) and (5) it follows for the relative change of the *T*-year quantile between years t_2 and t_1 at location *s*

$$\frac{Q_T(s,t_2)}{Q_T(s,t_1)} = \frac{\xi(s,t_2)}{\xi(s,t_1)} \cdot \frac{q_T(t_2)}{q_T(t_1)} = \exp[\xi_1 \cdot (t_2 - t_1)] \cdot \frac{q_T(t_2)}{q_T(t_1)}, \qquad t_2 \geq t_1 \geq t_0, \tag{8}$$

which does not depend on *s*.

The parameters of the model were estimated with the maximum likelihood (ML) method, using an R function for flexible GEV modeling written by Chris Ferro (University of Exeter, UK). Given *S* grid boxes in the region, the number of parameters in the model is *S*+5. Dealing usually with more than 50 grid boxes in one region it was extremely difficult to estimate all parameters simultaneously. Therefore, we applied a two-step procedure: in the first step we estimated all the site-specific location parameters $\xi_0(s)$ and in the second step we estimated the common regional parameters ($\xi_1, \gamma_0, \gamma_1, \kappa_0, \kappa_1$). These two steps were repeated until convergence.

2.3 Uncertainty and model checking

The ML method also provides standard errors of the estimates if the data are independent. In the case of spatial dependence the bootstrap can be used to assess the uncertainty of the parameters and quantiles of the distribution. Rather than bootstrapping the data of the grid boxes individually, the data for a certain year are bootstrapped simultaneously in order to preserve the spatial dependence. Prior to resampling, the trend has to be removed from the maxima *X*(*s*, *t*). This is done by the transformation (*Coles, 2001*):

$$\widetilde{X}(s,t) = \frac{1}{\hat{\kappa}(t)} \cdot \log\left[1 + \frac{\hat{\kappa}(t)}{\hat{\gamma}(t)} \cdot \left(\frac{X(s,t)}{\hat{\xi}(s,t)} - 1\right)\right], \tag{9}$$

where $\widetilde{X}(s,t)$ are the detrended seasonal maxima and $\hat{\xi}(s,t)$, $\hat{\gamma}(t)$ and $\hat{\kappa}(t)$ are the ML estimates of the GEV parameters. Then a sample $t_1,\ldots,t_i,\ldots,t_N$ is drawn with replacement from the years $1,\ldots,N$ (here the number *N* of years is 150). A bootstrap sample of detrended seasonal maxima is then obtained by taking the vector $\left(\widetilde{X}(1,t_i),\ldots,\widetilde{X}(s,t_i),\ldots,\widetilde{X}(S,t_i)\right)$ for each resampled year t_i. Finally, the sample is transformed back to the original scale and the parameters are re-estimated.

The transformed maxima $\widetilde{X}(s,t)$ should have a standard Gumbel distribution if the model is correct. This can be used for model checking, for example by visual comparison of empirical and theoretical distributions by means of probability and quantile plots.

3. Rhine basin

The river Rhine basin has an area of 185 000 km^2 and is situated in the territory of nine European countries (Fig. 1). The basin stretches from the Alps in the south with mountain peaks higher than 4000 m to a flat delta in the Netherlands in the north. The mean annual precipitation is quite variable – the wettest part is the Alpine region with more than 3000 mm of precipitation per year in some areas, the driest part is the area around Mainz in the centre of the Rhine basin where the mean annual precipitation is about 400 mm. The overall mean annual precipitation is 910 mm.

Fig. 1 The river Rhine basin (source: UNEP (2004) through UNEP/GRID-Europe).

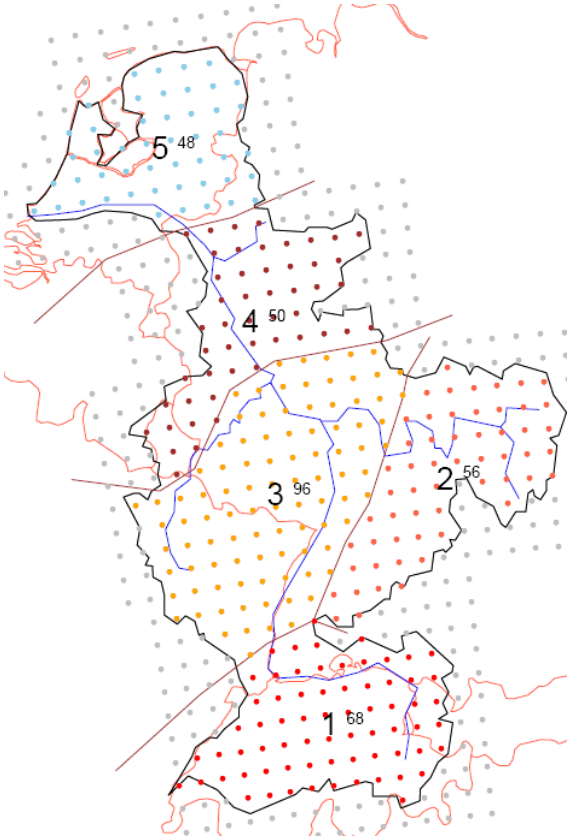

Fig. 2 Division of the river Rhine basin into five regions. The numbers in superscript give the number of grid boxes included in the region.

The precipitation maxima in the output of the KNMI regional climate model RACMO driven by the ECHAM5 global climate model under the SRES A1B emission scenario were studied. The RACMO-ECHAM5 run begins in 1950 and ends in 2100. The horizontal resolution of the RACMO model is about 25 km on a rotated longitude-latitude grid. There are 318 grid boxes whose centre lies within the Rhine basin (Fig. 2).

To use the index-flood model homogeneous regions have to be defined. Therefore we estimated the GEV parameters for the 1-day summer (JJA) and 5-day winter (DJF) maxima for two time slices (1950-1990 and 2060-2100), assuming no time dependence within these slices. We based the subdivision of the area on the spatial pattern of the dispersion coefficient exclusively, because the estimated shape parameter is less

accurate. Spatial heterogeneity of the dispersion coefficient turned out to be stronger for the summer maxima than for the winter maxima. We finally arrived at a subdivision of the Rhine basin into 5 regions (Fig. 2) each including 48 to 96 grid boxes. Region 1 roughly corresponds to the Swiss part of the basin and region 5 to the Dutch part.

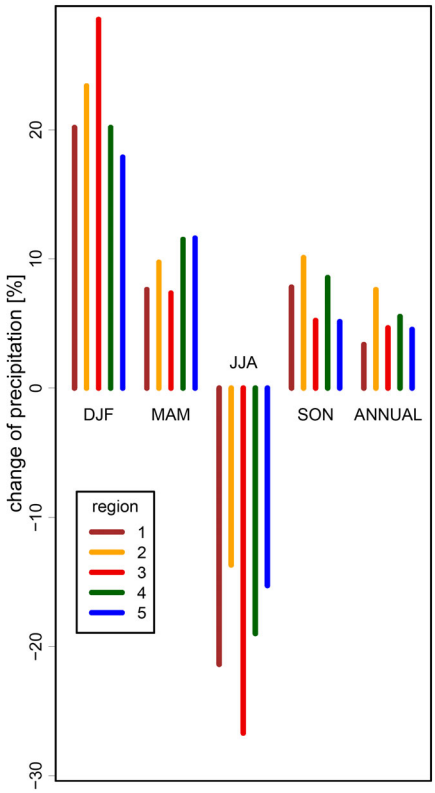

Fig. 3 Relative change of the seasonal and annual mean precipitation between the periods 1950-1990 and 2060-2100.

Fig. 3 shows the change of the seasonal and annual mean precipitation between the two time slices 1950-1990 and 2060-2100. In the model output the mean annual precipitation is increasing by about 5 percent over the whole basin, mean winter precipitation increases by more than 20 percent over most of the basin and mean summer precipitation decreases by 14-27 percent.

An important parameter in the non-stationary model, Eq.(5-7), is the start of the trend t_0. However, it is difficult to determine this parameter from the data of a single climate model run because of strong natural variability. To overcome this problem the data from the ESSENCE Project (http://www.knmi.nl/~sterl/Essence/) were used. In this project a large number of ECHAM5/MPI-OM AOGCM runs under the SRES A1B scenario were performed. These are the same global model and emission scenario as in the RACMO simulation for the ENSEMBLES project. We fitted the model $M_t = a + b \cdot (t - t_0)_+$ (with M_t the monthly precipitation, a, b the coefficients and t the year) for all months of the year, 17 ensemble members and 8 grid boxes lying more or less in the Rhine basin. Although, there was a considerable spread in the values of t_0 between both the ensemble members and the calendar months, we set t_0 to its mean value which was 1990.

To compare the RCM projections with observations we used the gridded observed daily precipitation amounts produced in ENSEMBLES work package WP5.1 (*Haylock et al., 2007*). The WP5.1 data set is available on different grids including a rotated longitude-latitude grid with resolution ~25 km, which makes the comparison with the RACMO data straightforward. The data cover the period from 1950 to 2006 and the records of about 2000 stations were used for gridding of precipitation data. In the Rhine basin the density of stations is variable, the highest coverage is found in the Netherlands (~1 station per 350 km^2).

4. Summer maxima

Fig. 4 shows boxplots of the parameters of the GEV model for the 1-day summer maximum precipitation in the RACMO-ECHAM5 simulation. These boxplots were obtained from 500 bootstrap samples. The upper panels present the values of the GEV parameters for the period before 1990, with no trend ($\xi_0, \gamma_0, \kappa_0$), the lower

panels give the trends ($\xi_1, \gamma_1, \kappa_1$). The estimate of $\bar{\xi}_0$ refers to the average ML estimate of $\xi_0(s)$ for all grid boxes in the region of interest.

Not surprisingly the location parameter in the Alpine area is markedly higher (more than 32 mm) than in the rest of the basin (about 21 mm). This is caused by the high precipitation amounts in the Alps. The dispersion coefficient varies between 0.32 and 0.37. The relatively high value of the dispersion coefficient in region 3 could be related to the low mean precipitation in this region. High values for the coefficient of variation of observed annual precipitation maxima have often been found in relatively dry areas, see *Brath et al. (2003)*. We do not have any explanation for the relatively high values of the dispersion coefficient in region 5. The shape parameter is positive (Fréchet distribution).

The parameters were also estimated for the 1-day summer maxima in the WP5.1 gridded data for the period of 1950-1990, assuming no trend. The results show that there is a systematic overestimation of the location parameter in the RACMO-ECHAM5 simulation of about 10 percent. The dispersion coefficient and the shape parameter are in most cases also somewhat larger in the RACMO-ECHAM5 simulation than in gridded observations.

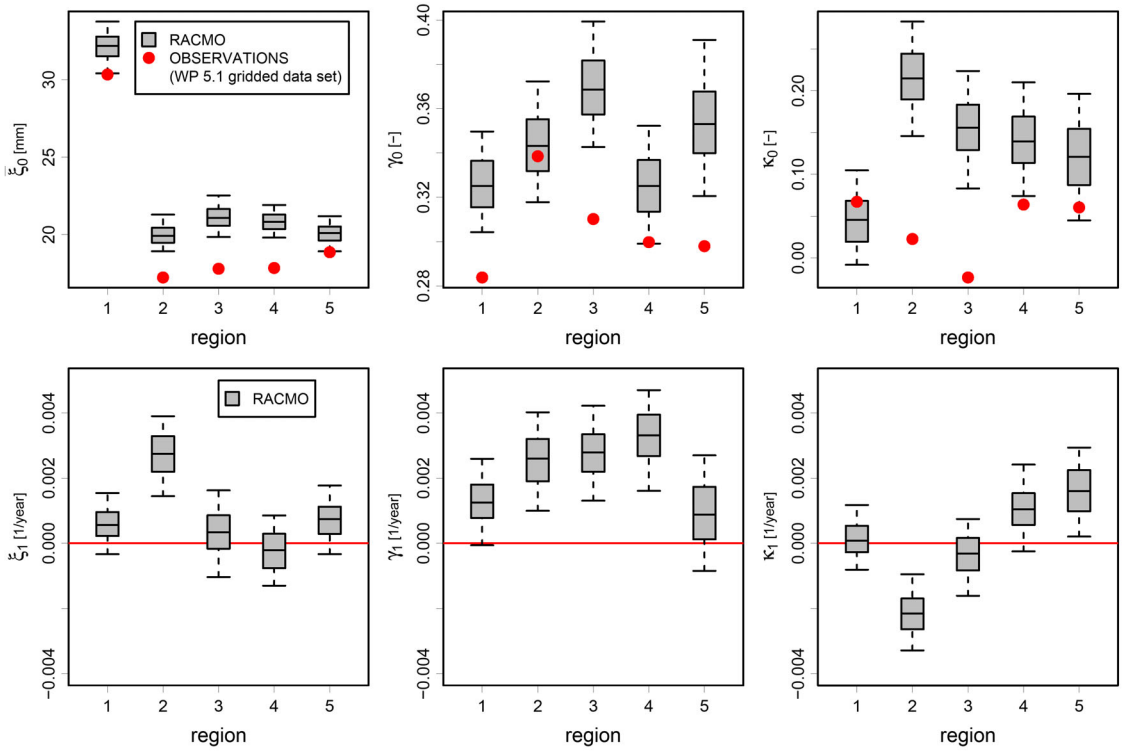

Fig. 4 Estimates of the parameters of the GEV model defined by Eq.(5-7) for the 1-day maximum precipitation in the summer season (JJA). The upper row gives estimates of the values of the GEV parameters for the years 1950-1990, the lower row represents the trends. The boxplots were obtained from 500 bootstrap samples. The boxes represent the interquartile range and the whiskers the 5th and 95th quantiles. The top left panel refers to the regional mean value of $\xi_0(s)$.

There is a notable positive trend in the dispersion coefficient in all five regions, whereas the trends in the location and the shape parameters are less clear. Relative

changes of quantiles of extremes are shown for the Swiss (in Fig. 5) and Dutch (in Fig. 6) parts of the Rhine basin. Despite the decrease of mean summer precipitation, the quantiles of the extremes increase. The increase in the 2-year quantile is mainly related to the slight increase of the location parameter in the two regions and is therefore rather small. Because of positive trend in the dispersion coefficient the relative increases of 50-year quantiles are much larger – up to 20 percent in the Swiss part and more than 50 percent in the Dutch part. For the later, the relative increase of the 50-year quantile is enforced by an increase of the shape parameter.

The uncertainty of the change of a given quantile is large, in general comparable with its magnitude. For the 50-year quantile this is partly caused by the uncertainty of the change of the shape parameter. The uncertainty of the change of this quantile can be reduced by assuming no trend in this parameter, i.e., $\kappa_1 = 0$. Fig. 7 compares the relative change of 50-year quantile in region 1 in the case of a constant shape parameter with that of a time dependent shape parameter. Although the uncertainty is reduced if κ is a priory set to zero, it is still high.

The goodness-of-fit was checked visually. We produced probability and quantile plots of the residuals $\tilde{X}(s,t)$ for all grid boxes in the Rhine basin. Fig. 8 gives these plots for two grid boxes in the Swiss part of the basin for the summer season. The left two plots refer to a grid box with a poor fit, the right two plots to a grid box with an adequate fit. For the whole Rhine basin 15 grid boxes with a poor fit were excluded and the model was fitted again. Figs. 4-7 refer to the refitted model.

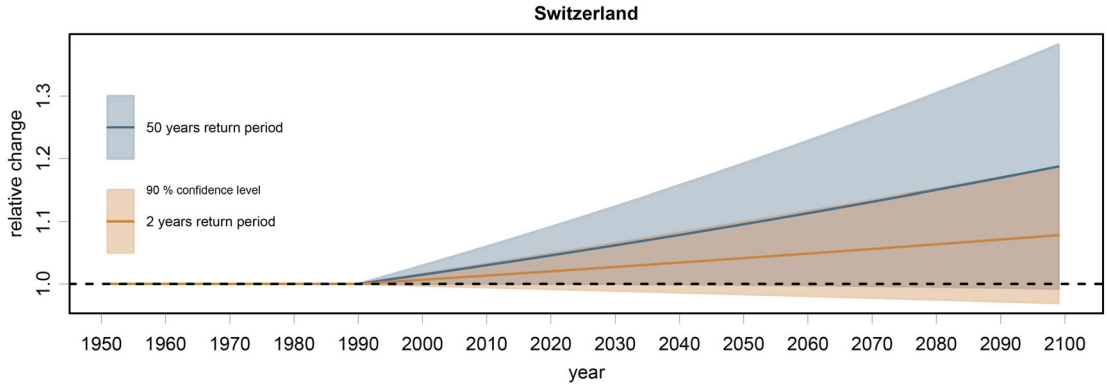

Fig. 5 Relative change of the 2- and 50-year quantile of 1-day summer maximum precipitation with 90 % confidence bands (JJA, region 1).

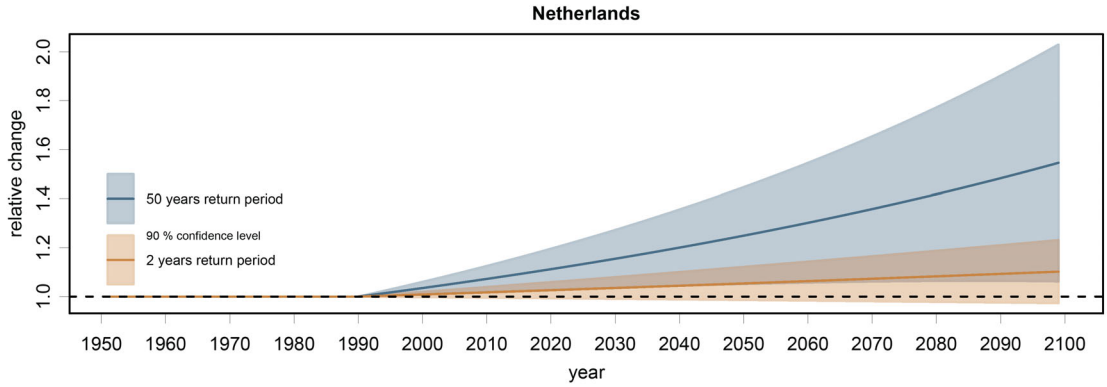

Fig. 6 Relative change of the 2- and 50-year quantile of 1-day summer maximum precipitation with 90 % confidence bands (JJA, region 5).

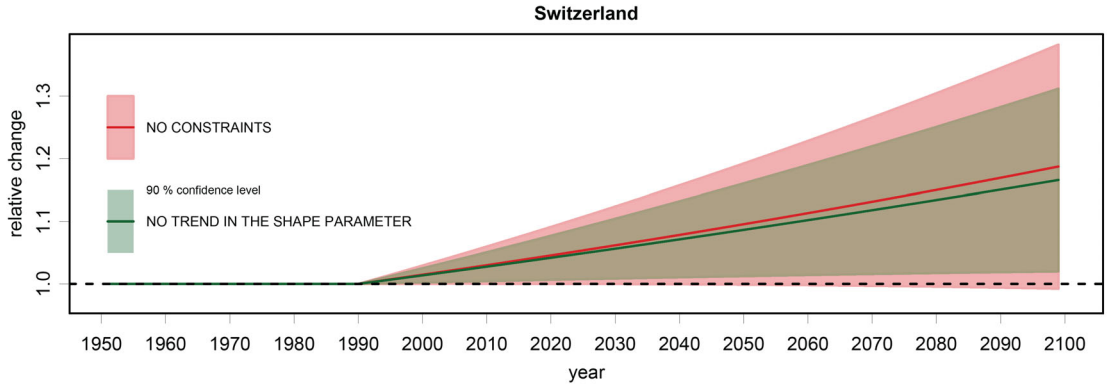

Fig. 7 Relative change of the 50-year quantiles of 1-day summer maximum precipitation for the unconstrained model and the model with no trend in the shape parameter (JJA, region 1).

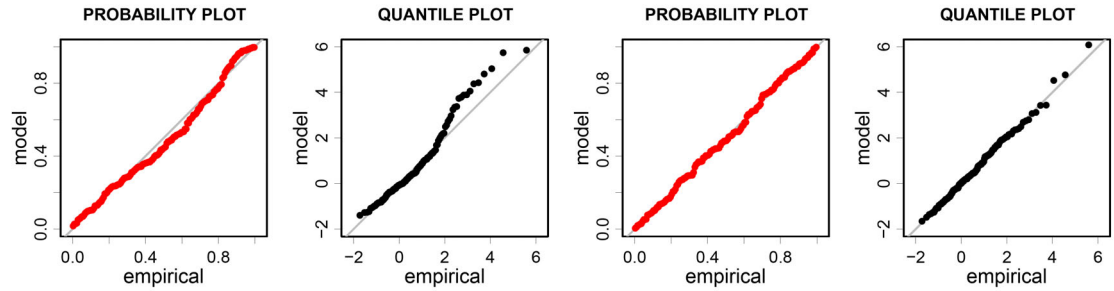

Fig. 8 Diagnostic plots for two grid boxes in the Swiss part of the basin for the summer season. The empirical probabilities/quantiles of the transformed maxima (Eq.9) are compared with those of the standard Gumbel distribution. The left two plots refer to one of the excluded grid boxes, the right two plots to a grid box with proper fit.

5. Winter maxima

Fig. 9 shows boxplots of the parameters of the GEV model for the 5-day winter maximum precipitation amounts. As for the summer season the location parameter in the Alpine region is higher than in the rest of the basin. The dispersion coefficient shows a south-north gradient. The shape parameter is almost zero in three of the five regions.

Compared to the gridded observations the RACMO-ECHAM5 simulation overestimates the location and the shape parameters. A more serious point is the large underestimation of the dispersion coefficient in the RACMO-ECHAM5 simulation.

The location parameter increases in time and the shape parameter decreases in time over the whole area, whereas there is almost no change in the dispersion coefficient.

Fig. 10 gives the relative change of the 2- and 50-year quantiles of the extremes for the Swiss part of the basin. Due to the increase of the location parameter the 2-year quantile increases. The relative increase in these quantities is, however, only about half the relative increase in mean winter precipitation. For the 50-year quantile the effect of the increase of the location parameter is counterbalanced by the decrease of the shape parameter resulting in almost no change in this quantile.

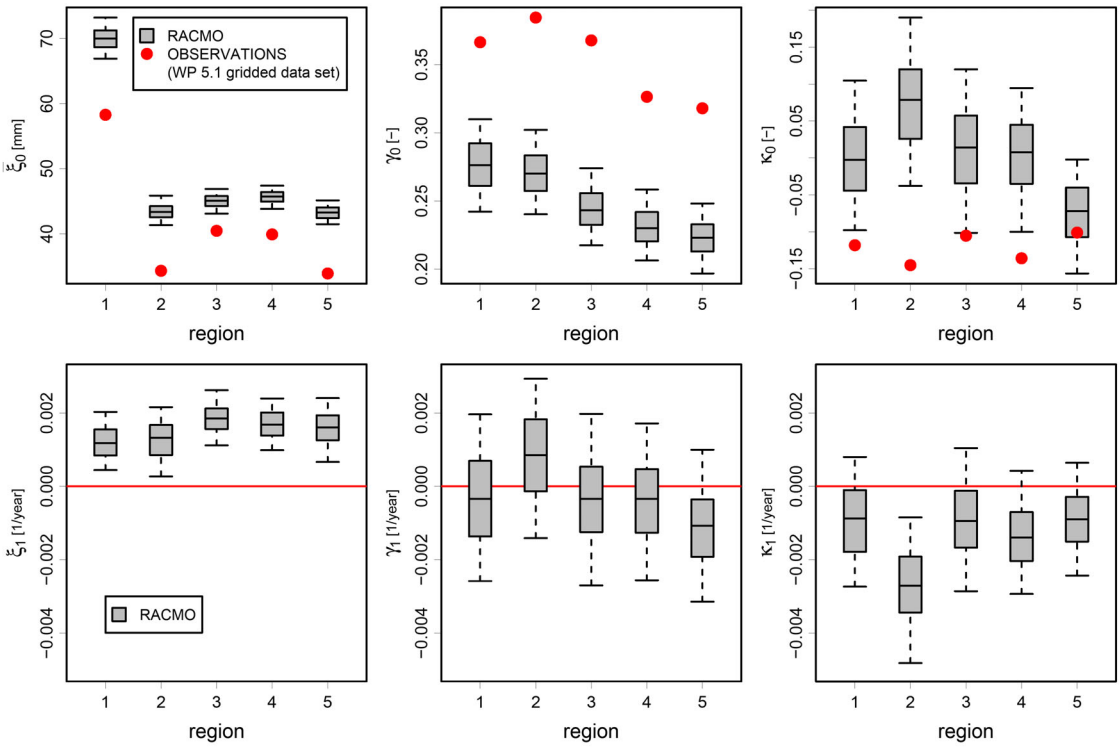

Fig. 9 Same as Fig. 4 but for the 5-day precipitation maxima in the winter season (DJF).

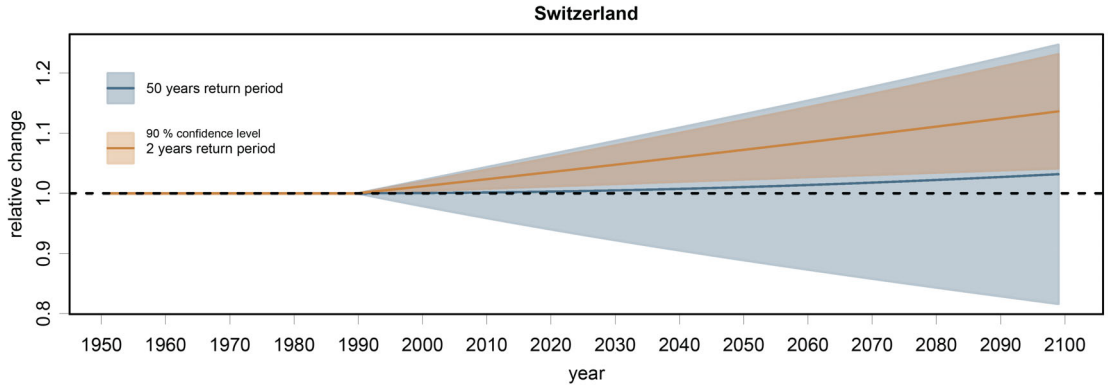

Fig. 10 Relative change of the 2- and 50-year quantile of 5-day maximum precipitation with 90 % confidence band (DJF, region 1).

6. Conclusion and discussion

Regional GEV modeling provides an informative summary of changes in the GEV parameters and various quantiles of the extremes. It gives more insight into the changes of precipitation extremes and the differences between simulated and observed precipitation maxima than looking at a single quantile only. In addition, the standard errors of estimated common parameters are significantly reduced compared to the estimates based on the data of an individual grid box (~ 70% for ξ_0 and ξ_1, ~ 55% for γ_0 and γ_1 and ~ 35% for μ_0 in the case of JJA).

The most evident changes of the GEV parameters in the RACMO-ECHAM5 simulation are the positive trend in the dispersion coefficient of the 1-day maxima in summer and the positive trend in the location parameter of the 5-day maxima in winter. For the winter maxima there is an indication of a decrease of the shape parameter as well.

Despite the reduction of standard errors due to regional pooling of data, the changes in the quantiles of the extreme-value distributions are often not statistically significant. For the 2-year quantile of the 1-day summer maxima this can be attributed to the fact that the change in location parameter is small in the two regions considered. The estimates of the relative changes of the 50-year quantiles are strongly affected by the estimates of the dispersion coefficient and the shape parameter, which have large standard errors. In the summer season there is evidence of a heterogeneous change of the shape parameter over the river Rhine basin. A significant increase in this parameter is found in the northern regions 4 and 5, which leads to a large, uncertain, increase of the 50-year quantile in these regions. Ignoring a possible change in the shape parameter, as is often done in the literature, results in a much more uniform increase in the 50- year quantile across the river basin. This increase is mainly due to the increase of the dispersion coefficient in summer. Despite the large increase of mean winter precipitation there is no evidence of a change of the 50-year quantile in the winter.

With the exception of a serious underestimation of the dispersion coefficient of the 5-day winter maxima, the estimated GEV parameters for present-day conditions in the RACMO-ECHAM5 simulation were not much different from those for the ENSEMBLES WP5.1 gridded data. Part of the differences may be due to the low density of the station network used for gridding. For the Swiss part of the basin a comparison will be made with the extremes in the Alpine data set (*Frei and Schär, 1998*), which is based on much more stations in this region than the WP5.1 data set.

The goodness-of-fit was explored visually. An objective test is desirable, e.g., using the Kolmogorov-Smirnov or Anderson-Darling statistics. This requires an extension of the bootstrap in Section 2.3 to determine the statistical significance of these statistics.

Other covariates than the year t could be used to describe the change of the GEV parameters. In fact, using a covariate such as global mean temperature of the forcing GCM instead of the year avoids the difficulty with determining the start of the trend. This idea will be explored further.

References

Adlouni, S.El., Ouarda, T.B.M.J., Zhang, X., Roy, R., Bobée, B., 2007. Generalized maximum likelihood estimators for the nonstationary generalized extreme value model. Water Resources Research 43, W03410, doi:10.1029/2005WR004545.

Alila, Y., 1999. A hierarchical approach for the regionalization of precipitation annual maxima in Canada. Journal of Geophysical Research 104, 645-655.

Brath A., Castellarin, A., Montanari, A., 2003. Assessing the reliability of regional depth-duration-frequency equations for gaged and ungaged sites, Water Resources Research 39 (12), 1367, doi:10.1029/2003WR002399.

Buonomo, E., Jones, R., Huntingford, C., Hannaford, J., 2007. On the robustness of changes in extreme precipitation over Europe from two high resolution climate change simulations. Quarterly Journal of the Royal Meteorological Society 133, 65-81.

Christensen, O.B., Christensen, J.H., 2004. Intensification of extreme European summer precipitation in a warmer climate, Global and Planetary Change 44, 107-117.

Coles, S., 2001. An Introduction to Statistical Modeling of Extreme Values. Springer-Verlag, New York.

Cunderlik, J.M., Burn, D.H., 2003. Non-stationary pooled flood frequency analysis. Journal of Hydrology 276, 210-223.

Cunderlik, J.M., Ouarda, T.B.M.J., 2005. Regional flood-duration-frequency modeling in the changing environment. Journal of Hydrology 318, 276-291.

Ekström, M., Fowler, H.J., Kilsby, C.G., Jones, P.D., 2005. New estimates of future changes in extreme rainfall across the UK using regional climate model integrations. 2. Future estimates and use in impact studies. Journal of Hydrology 300, 234-251.

Fowler, H.J., Ekström, M., Kilsby, C.G., Jones, P.D., 2005. New estimates of future changes in extreme rainfall across the UK using regional climate model integrations, 1. Assessment of control climate. Journal of Hydrology 300, 212-233.

Frei C., Schär, C., 1998. A precipitation climatology of the Alps from high-resolution rain-gauge observations. International Journal of Climatology, 18, 873-900.

Frei, Ch., Schär, Ch., 2001. Detection probability of trends in rare events: Theory and application to heavy precipitation in the Alpine region. Journal of Climate 14, 1568-1584.

Frei, C., Schöll, R., Fukutome, S., Schmidli, J., Vidale, P.L., 2006. Future change of precipitation extremes in Europe: Intercomparison of scenarios from regional climate models. Journal of Geophysical Research, 111, D06105, doi10.1029/2005JD005965.

García, J.A., Gallego, M.C., Serrano, A., Vaquero, J.M., 2007. Trends in block-seasonal extreme rainfall over the Iberian Peninsula in the second half of the twentieth century. Journal of Climate 20, 113-130.

Goubanova, K., Li, L., 2007. Extremes in temperature and precipitation around the Mediterranean basin in an ensemble of future climate scenario simulations. Global and Planetary Change 57, 27-42.

Haylock, M.R., Hofstra, N., Klein Tank, A.M.G., Klok, E.J., Jones, P.D., New, M., 2007. A European daily high-resolution gridded dataset of surface temperature and precipitation. Journal of Geophysical Research (submitted).

Huntingford, C., Jones, R.G., Prudhomme, C., Lamb, R., Gash, J.H.C, Jones, D.A., 2003. Regional climate model predictions of extreme rainfall for a changing climate. Quarterly Journal of the Royal Meteorological Society 129, 1607-1621.

Kharin, V.V., Zwiers, F.W., 2005. Estimating extremes in transient climate change simulations. Journal of Climate 18, 1156-1173.

Kyselý, J., Picek, J., 2007. Regional growth curves and improved design value estimates of extreme precipitation events in the Czech Republic. Climate Research 33, 243-255.

Renard, B., Garreta, V., Lang, M., 2006. An application of Bayesian analysis and Markov chain Monte Carlo methods to the estimation of a regional trend in annual maxima. Water Resources Research 42, W12422, doi:10.1029/2005WR004591.

Schaefer, M.G., 1990. Regional analyses of precipitation annual maxima in Washington State. Water Resources Research 26 (1), 119-131.

Sen, P.K., 1968. Estimation of the regression coefficient based on Kendall's tau. Journal of the American Statistical Association 63, 1379 – 1389.

UNEP, 2004. Freshwater in Europe - Facts, Figures and Maps.